21st IMEKO TC4 International Symposium and
19th International Workshop on ADC Modelling and Testing
Understanding the World through Electrical and Electronic Measurement
Budapest, Hungary, September 7-9, 2016

# Periodic signal parameters' estimations from random sampling measurements under non-coherent sampling condition

Dušan Agrež

*University of Ljubljana, Faculty of Electrical Engineering,*
*Tržaška 25, Ljubljana, Slovenia, dusan.agrez@fe.uni-lj.si,* +386 1 4768 250

***Abstract* – Paper presents estimations of the periodic signal parameters in the case of random sampling and under non-coherent sampling condition where randomization of sampling intervals shapes the noise floor in the sampled spectrum with addition of spectral leakage. To achieve the lowest estimation errors the non-parametric interpolated DFT estimation of frequency should be used first for detection of the signal component and after that iterative 4-parametric sine-fit algorithm should be used for other parameters. In any case of estimation, the relative number of random samples has to be at least 0.1.**

***Keywords* – periodic signal, parameter estimation, random sampling, non-coherent sampling condition**

## I. INTRODUCTION

In many applications of practical interest, we often wish to estimate signal parameters and reconstruct a signal (a discrete signal, a discrete image, etc.) from incomplete time samples, which can be attained nonuniformly and randomly [1],[2]. Unlike the uniform sampling case, where the aliases are simply periodic replicas of the signal original spectrum, random sampling theory shows that the randomization of sampling intervals shapes the aliases into a noise floor in the sampled spectrum [3].

Fig. 1 shows sinusoidal signal $g$, which can be generally expressed as $w(n t_S)\cdot\sum_{m=0}^{M-1} A_m \sin(2\pi f_m n t_S + \varphi_m)$ ($f_m$, $A_m$, and $\varphi_m$ are frequency, amplitude, and phase of the particular component), for one component presented by randomly sampled points with low 'duty ratio' $D_{rs} = N_{rs}/N$, where $N_{rs}$ is the number of random samples from among total of $N$ samples in the non-coherent measurement interval $T_M = N t_S$. Basic raster of $N$ samples is equidistant with sampling interval $t_S$ [4]. Estimations of the component signal parameters are distorted due to the missing samples in the time domain [5] or due to large random sampling noise in the frequency domain (Fig. 2 - line b) where *SNR* for investigated component is very low when $D_{rs}$ is low. Considering also the non-coherent sampling condition with leakage effect, where measurement interval $T_M$ is not an integer multiple of the signal period $\theta_m = T_M/T_m = i_m + \delta_m$, parameters estimations are not an easy task [6],[7]. The leakage signal energy additionally spread along the frequency axis and disturb the DFT coefficients (Fig. 2), which can not be removed as in the case of compressive sensing with coherent sampling model [8],[9].

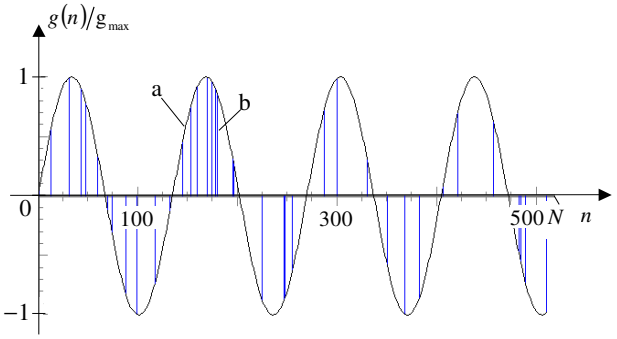


*Fig. 1. Signals of random sampling: a – original signal, b – random sampled signal; $N = 512$, $\theta = 3.8$, $A = 1$, $\varphi = 0$, $D_{rs} \doteq 0.074$*

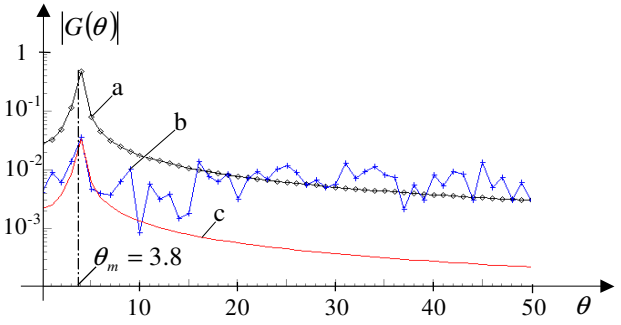


*Fig. 2. Spectra of signals from Fig. 1: a – original signal, b – random sampled signal $D_{rs} \doteq 0.074$, c – reconstructed signal*

## II. ANALYSIS FOR PARAMETERS' ESTIMATIONS

Accurate measurement of a multisine waveform is a

classic problem in spectral analysis. It is well known that non-parametric algorithms based on the discrete Fourier transform (DFT) have to contend with spectral leakage, which affects both amplitude estimation accuracy and frequency resolution [10]. These methods usually estimate the signal component frequency as key parameter by searching for the maximum in the spectrum by using DFT [11]. Advanced windowed functions and interpolation schemes have been applied to compensate for the effects of leakage caused by incoherent sampling and finite frequency resolution problems [12], respectively. It is also common knowledge that approaches based on a parametric signal model, can achieve much better frequency resolution, but this is obtained at the price of greater complexity [13].

For estimations of the signal parameters from sparse sampled periodic signal two methods are investigated and compared: the non-parametric interpolated DFT and the sine-fit parametric approach [14]. In the first approach, one can choose the number of DFT coefficients in interpolation and the window function w(*) [12], in the second approach, a number of parameters has to be defined: non-iterative 3-parametric sine-fit estimation when component frequency is known or 4-parametric estimation when also the frequency has to be estimated in the iterative procedure [13].

In the first approach typically two or three largest DFT coefficients $G(i_m-1)$, $G(i_m)$, $G(i_m+1)$ and Rife-Vincent windows class I with suitable order $P$ are used [12]:

- Two-point frequency estimation where $s$ is a sign of displacement $\delta_m$:

$$\theta_m = i_m +_2\delta_m \doteq i_m + s\frac{(P+1)\cdot|G(i_m+s)| - P\cdot|G(i_m)|}{|G(i_m)|+|G(i_m+s)|} \quad (1)$$

- Three-point frequency estimation:

$$\theta_m = i_m + \delta_m \doteq i_m + (P+1)\cdot\frac{|G(i_m+1)|-|G(i_m-1)|}{|G(i_m-1)|+2|G(i_m)|+|G(i_m+1)|} \quad (2)$$

- One-point amplitude estimation:

$${}_1A_m \doteq 2\left|\frac{2^{2P}}{(2P)!}\cdot\frac{\pi\delta_m}{\sin(\pi\delta_m)}\cdot\prod_{l=1}^{P}\left(l^2-\delta_m^2\right)\right||G(i_m)| \quad (3)$$

- Three-point amplitude estimation:

$${}_3A_m \doteq 2\left|\frac{2^{2P}}{(2P+2)!}\cdot\frac{\pi\delta_m}{\sin(\pi\delta_m)}\cdot\prod_{l=1}^{P+1}\left(l^2-\delta_m^2\right)\right| \cdot\left(|G(i_m-1)|+2|G(i_m)|+|G(i_m+1)|\right) \quad (4)$$

- Three-point phase estimation with the arguments of the three largest local DFT coefficients $\varphi_{i_m} = \arg[G(i_m)]$:

$${}_3\varphi_m = \frac{(1-\delta_m)\varphi_{i_m-1}+4\varphi_{i_m}+(1+\delta_m)\varphi_{i_m+1}}{6} - \frac{2a\delta_m}{3}+\frac{\pi}{2} \quad (5)$$

Since the sparse sampling very increase the noise in the frequency domain (Fig. 2) it is not suitable to increase the number of interpolation DFT coefficients in interpolations due to their distortions. Fig. 3 shows the mean values of the absolute relative errors of the amplitude DFT coefficients ( $e|G_{\text{rs}}(i_m)|$, $e|G_{\text{rs}}(i_m+1)|$, and $e|G_{\text{rs}}(i_m-1)|$ ) around the local peak in relation to original spectrum on $N=512$ samples normalized by the duty ratio $|G(i)|^* = |G(i)|\cdot D_{\text{rs}}$ in (6) (Fig. 2 - line c).

$$e\left(|G_{\text{rs}}(i)|\right) = \frac{|G_{\text{rs}}(i)|-|G(i)|^*}{|G(i)|^*} \quad (6)$$

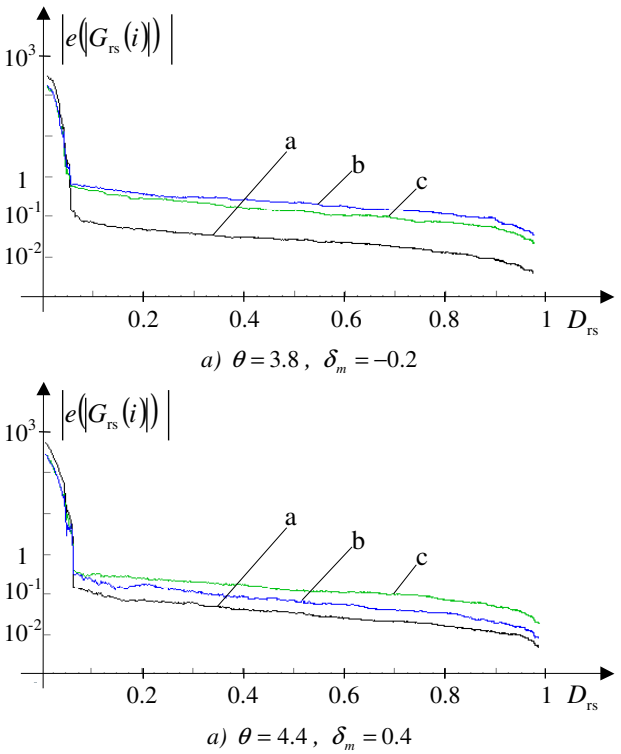


*Fig. 3. Mean values of the absolute relative errors of the amplitude DFT coefficients; a – $e|G_{\text{rs}}(i)|$, b – $e|G_{\text{rs}}(i+1)|$, c – $e|G_{\text{rs}}(i-1)|$, $A=1$, $\varphi = 0\,\text{deg}$, $N_{\text{repeat}} = 100$ trials*

Analyses in Fig. 3 shows that it is better to use two-point estimation for frequency to determining the position of the measurement component $\delta_m = \theta_m - i_m$ between DFT coefficients $G(i_m)$ and $G(i_m+1)$ surrounding the component $m$ as the key parameter due specific distortion in sparse sampling. This conclusion can be supported also by analysing of error characteristics using two and three- point estimations (Fig. 4) [12].

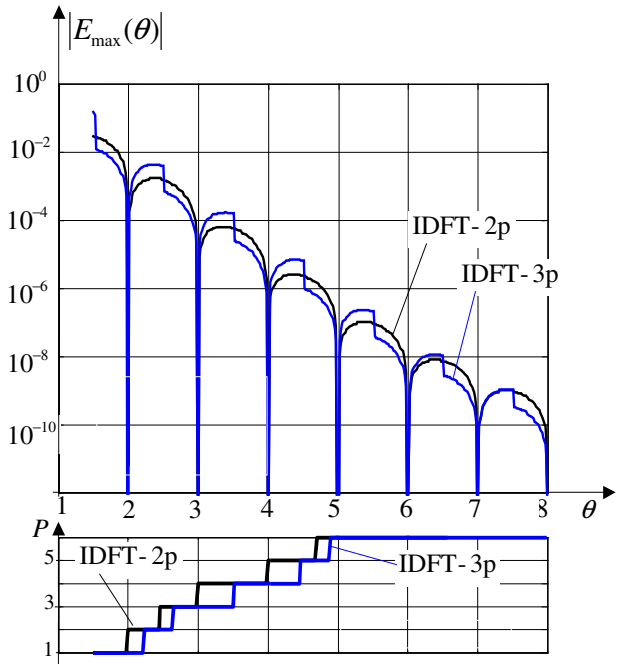


*Fig. 4. Minimal curves of the maximal errors of the frequency estimations with the two- (IDFT-2p) and three- (IDFT-3p) interpolations of the DFT using RV-I windows and the corresponding orders $P = 1...6$*

Fig. 4 shows collected minimal curves of the maximal bias errors of the frequency estimations due to phase changing with the two-point (IDFT-2p) and three-point (IDFT-3p) interpolations of the DFT using RV-I windows and the corresponding orders $P = 1...6$ with which these minimal values have been obtained. It can be seen that bias errors are on the same level with two (1) or three-point (2) estimations except window order $P$ has to be increased with two-point estimation.

Whenever there is no information of frequency content of the signal, the component frequency estimation is the first step and the key to estimate other parameters (amplitude, phase, and sometimes also damping) and this is valid both for parametric and non-parametric approach. Results in Figs. 5 and 6 confirm above presumptions, where frequency estimation error is defined as $|E(\theta)| = |\theta_{est.} - \theta_{true}|$.

It can be noticed that the relative number of random samples $D_{rs} = N_{rs}/N$ has to increase at least to 0.1 when the frequency estimation errors step-like drop below 0.1 bin but this is still far from the target values when we have the whole ensemble of samples (Figs. 5 - line a and 6 - line a). With increasing $D_{rs}$ errors slowly drop but iterations in process of randomly adding additional samples relatively very increase (for $N = 512$ we typically need 2000 iterations to achieve $D_{rs} \approx 0.98$). Due to the randomness, some positions may be repeatedly sampled, whereas other positions are left blank.

Parametric estimation approach (Fig. 5 - line c: 4-parametric estimation with 9 iterations) gives better results than the non-parametric IDFT approach (Fig. 5 - line b and 5 - line d) but frequency has to be estimated first (typically by symmetric 3-point estimation using the Hann window $P = 1$ and (2)). If we don't have good initial value of the component frequency the parametric approach gives useless results (Fig. 6 - line c).

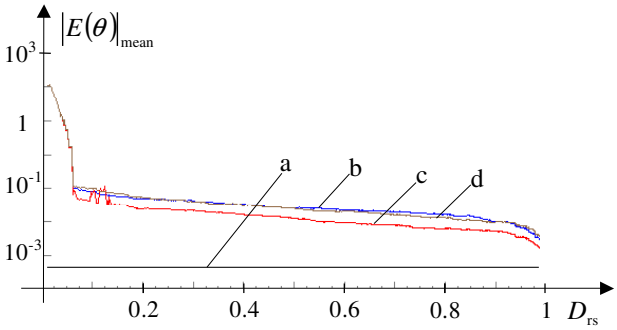


*Fig. 5. Mean values of the absolute errors of the frequency estimation; a – original signal – IDFT(f-3p), b – random sampled signal – IDFT(f-3p), c – random sampled signal – 4-par. sine-fit (start with estimated f-3p), d – random sampled signal – IDFT(f-2p), $\theta = 3.8$, $A = 1$, $\varphi = 0\text{deg}$, $N_{repeat} = 100$ trials*

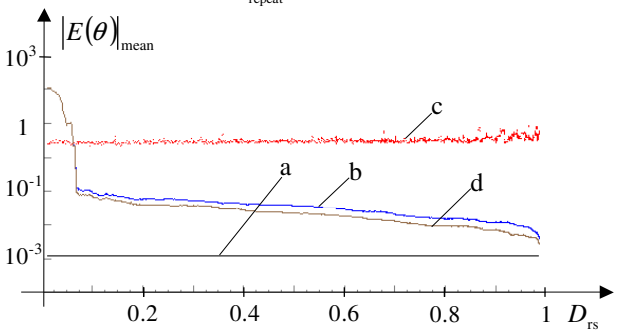


*Fig. 6. Mean values of the absolute errors of the frequency estimation; a – original signal – IDFT(f-3p), b – random sampled signal – IDFT(f-3p), c – random sampled signal – 4-par. sine-fit (start with $\theta = 2$), d – random sampled signal – IDFT(f-2p), $\theta = 4.4$, $A = 1$, $\varphi = 0\text{deg}$, $N_{repeat} = 100$ trials*

After the point where component arise out of the random sampling noise (Fig. 2 - line b: $D_{rs} \doteq 0.074$) two-point IDFT estimation (Figs. 5 - line d and 6 - line d) gives lower errors than the three-point estimation and especially in the case of large non-coherency (Fig. 6 - line d: $\delta_m = 0.4$).

The same behavior of the estimation errors can be noticed also for the amplitude (Figs. 7 and 9) and phase estimations (Fig. 8) where the same testing conditions were used as in Figs. 5 and 6. Errors drop very fast at the beginning of the $D_{rs}$ increasing and after the point around $D_{rs} \approx 0.1$ these behaviours changed to slowly decreasing.

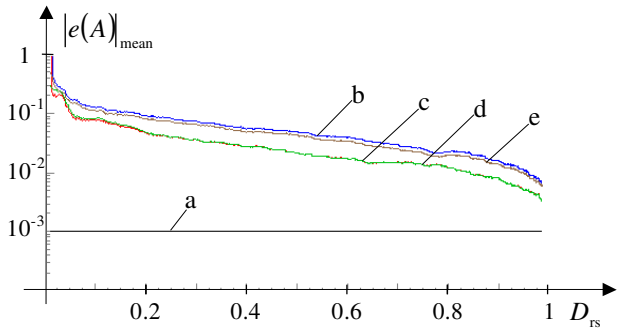


*Fig. 7. Mean values of the relative errors of the amplitude estimation; a – original signal – IDFT(f-3p, A-3p), b – random sampled signal – IDFT(f-3p, A-3p), c – random sampled signal – 4-par. sine-fit (start with estimated f-3p), d – random sampled signal – 3-par. sine-fit (f-3p), e – random sampled signal – IDFT(f-2p, A-1p), $\theta = 3.8$, $A = 1$, $\varphi = 0\,\text{deg}$, $N_{\text{repeat}} = 100$ trials*

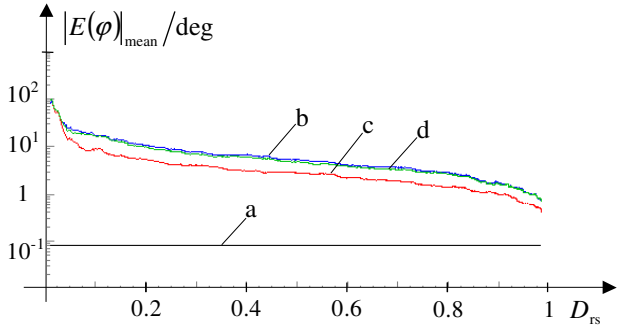


*Fig. 8. Mean values of the absolute errors of the phase estimation; a – original signal – IDFT(f-3p, ph-3p), b – random sampled signal – IDFT(f-3p, ph-3p), c – random sampled signal – 4-par. sine-fit (start with estimated f-3p), d – random sampled signal – 3-par. sine-fit (f-3p), $A = 1$, $\theta = 3.8$ $N_{\text{repeat}} = 100$ trials*

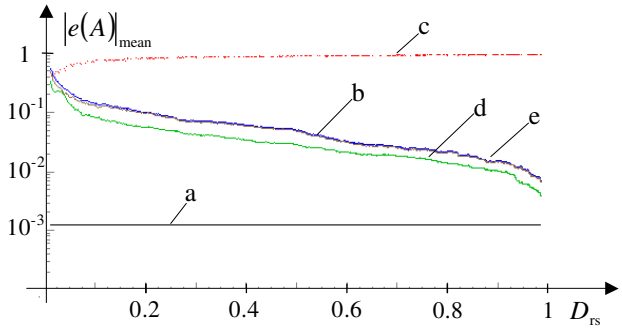


*Fig. 9. Mean values of the relative errors of the amplitude estimation; a – original signal – IDFT(f-3p, A-3p), b – random sampled signal – IDFT(f-3p, A-3p), c – random sampled signal – 4-par. sine-fit (start with $\theta = 2$), d – random sampled signal – 3-par. sine-fit (f-3p), e – random sampled signal – IDFT(f-2p, A-1p), $\theta = 4.4$, $A = 1$, $\varphi = 0\,\text{deg}$, $N_{\text{repeat}} = 100$ trials*

Iterative 4-parametric estimation (Figs. 7 - line c and 8 - line c) gives better result than one-step 3-parametric estimation (Fig. 8 - line d) but initial frequency has to be very good estimated. If we fix the value of the estimated frequency by IDFT the one step 3-parametric sine-fit estimation gives the error values as with non-parametric approach (Fig. 8 - line d).

## III. EXPERIMENTAL RESULTS

To demonstrate the behaviour of estimations of the periodic signal parameters in the case of random sampling and under non-coherent sampling condition in real measurement environment a digitizing oscilloscope (DO), Agilent 54501A [15] was used, to randomly acquire signal generated by a stable voltage generator, Keysight 33500B [16], with a nominal sine voltage of the amplitude $A_{\text{v}} = 0.900\,\text{V}$.

First, the signal frequency was fixed to $f_{\text{v}} = 1.9\,\text{MHz}$ and with time constant of $c_{\text{time}} = 200\,\text{ns/div}$ and 10 divisions in the x-axis, DO acquire and shows 3.8 periods of signal in the duration of $T_{\text{M}} = 2\,\mu\text{s}$ ($\theta = f_{\text{v}} \cdot T_{\text{M}} = 1.9\,\text{MHz} \cdot 2\,\mu\text{s} = 3.8$). Since the DO display use $N = 500$ points to represents the signal in the x-axis the equivalent sampling frequency was $f_{\text{S,eq}} = T_{\text{M}}/N = 250\,\text{MHz}$ what is 25-times larger than the DO real sampling frequency $f_{\text{S}} = 10\,\text{MHz}$ and sampling points were acquired with the multiple 'randomly triggered' sweeps to fill the points for display presentation [15]. To fulfil all $N = 500$ points typically 150 sweeps were needed and this acquisition procedure was controlled remotely by SCPI commands: :TIM:MODE SING and :RUN [15].

Figs. 10 (frequency estimation) and 11 (amplitude estimation) show estimation errors where parameter's reference value is that attained with estimation on the whole number of the filled points $D_{\text{rs}} = 1$ after 150 sweeps with 3-point estimations ((2) and (4)).

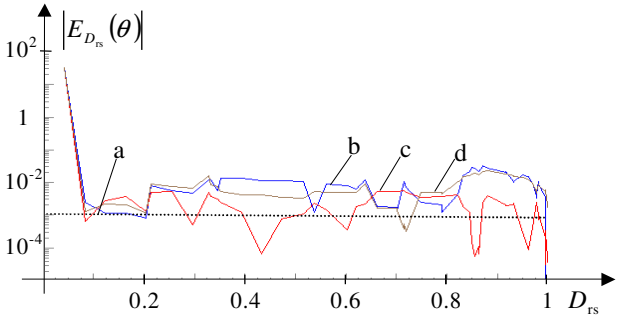


*Fig. 10. Mean values of the maximal absolute errors of the frequency estimation; a – target estimation error, b – random sampled signal – IDFT(f-3p), c – random sampled signal – 4-par. sine-fit (start with estimated f-3p), d – random sampled signal – IDFT(f-2p), $\theta = 3.8$, $\varphi \approx 0\,\text{deg}$, $N_{\text{sweeps}} = 150$*

Estimation errors are defined as $\left|E_{D_{\mathrm{rs}}}(\theta)\right| = \left|\theta_{\mathrm{est},D_{\mathrm{rs}}} - \theta_{3\mathrm{p},D_{\mathrm{rs}}=1}\right|$ for the relative frequency (Fig. 10) and as $\left|e_{D_{\mathrm{rs}}}(A)\right| = \left|A_{\mathrm{est},D_{\mathrm{rs}}} / A_{3\mathrm{p},D_{\mathrm{rs}}=1} - 1\right|$ for the amplitude (Fig. 11).

Estimation error behaviors in Fig. 10 confirm simulation results from Figs. 5 and 6 with very fast decrease at low values of $D_{\mathrm{rs}} < 0.1$ to the target level (Fig. 10 – line a: $\left|E_{D_{\mathrm{rs}}}(\theta)\right| = 10^{-3}$) and after increasing $D_{\mathrm{rs}} > 0.1$ errors drop slowly to final estimation result with the whole ensemble of points at $D_{\mathrm{rs}} = 1$.

The same estimation error behaviors can be noticed also in the case of the amplitude estimation (Fig. 11). The best results perform parametric sine-fit estimation procedures where initial frequency was estimated first by the 3-point interpolated DFT approach (2).

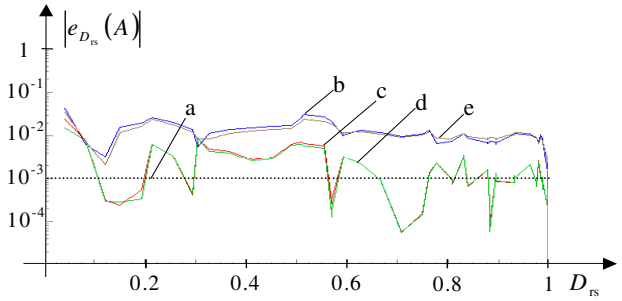


*Fig. 11. Mean values of the maximal relative errors of the amplitude estimation; a – target estimation error, b – random sampled signal – IDFT(f-3p, A-3p), c – random sampled signal – 4-par. sine-fit (start with estimated f-3p), d – random sampled signal – 3-par. sine-fit (f-3p), e – random sampled signal – IDFT(f-2p, A-1p), $\theta = 3.8$, $\varphi \approx 0\,\mathrm{deg}$, $N_{\mathrm{sweeps}} = 150$*

To analyse the estimation error behavior when the relative frequency is changing the testing conditions from Fig. 10 were enhanced from one frequency of $\theta = 3.8$ to frequency range $\theta = 1.4 \div 6$ with frequency increment $\Delta\theta = 0.05$ (Fig. 12).

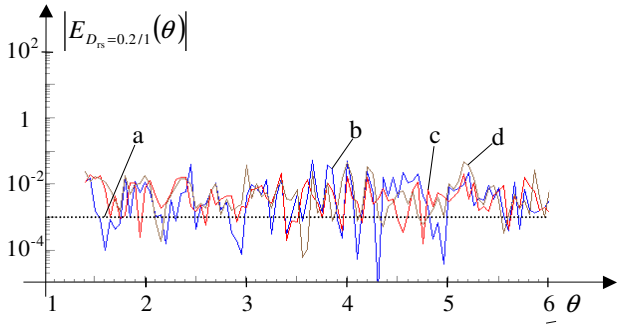


*Fig. 12. Mean values of the maximal absolute errors of the frequency estimation; a – target estimation error, b – random sampled signal – IDFT(f-3p), c – random sampled signal – 4-par. sine-fit (start with estimated f-3p), d – random sampled signal – IDFT(f-2p), $\varphi \equiv 0\,\mathrm{deg}$, $N_{\mathrm{sweeps}} = 150$*

For this testing the signal frequency was changed from $f_{\mathrm{v,min}} = 0.7\,\mathrm{MHz}$ to $f_{\mathrm{v,max}} = 3.0\,\mathrm{MHz}$ with step $\Delta f_{\mathrm{v}} = 25\,\mathrm{kHz}$ and at each frequency the estimation error was defined as difference between estimation value around $D_{\mathrm{rs}} = 0.2$ and estimation value when $D_{\mathrm{rs}} = 1$ (Fig. 12: $\left|E_{D_{\mathrm{rs}}=0.2/1}(\theta)\right| = \left|\theta_{\mathrm{est},D_{\mathrm{rs}}=0.2} - \theta_{\mathrm{est},D_{\mathrm{rs}}=1}\right|$). The frequency estimation errors from Fig. 12 show that with changing the relative frequency the relation of errors between estimations with low sampling duty cycle and estimations with the whole ensemble of points remain on the same level.

## IV. CONCLUSIONS

The paper shows that parameters' estimations of randomly and non-coherently sampled signals are more problematic than in the case of coherency where problem of frequency estimation is much reduced like in approaches of compressive sensing. To achieve the lowest estimation errors the non-parametric IDFT estimation of frequency should be used first for detection of component frequency and after that iterative parametric method should be used for other parameters.

Simulation and experimental results show that the parameters' estimations are possible when duty ratio of random samples from among total samples in the non-coherent measurement interval is very low: from 0.1 to 0.2. With these duty ratios of random samples it is possible to achieve error levels of 0.001 bins of the frequency estimations in relation to the estimation on full ensemble of points. The same relative error level (0.001) of the best estimation with full points can be achieved also for the amplitude estimation using reduced duty ratio of 0.1.

## *REFERENCES*


[1] Y. Zhao, Y. H. Hu, H. Wang, "Enhanced random equivalent sampling based on compressed sensing." IEEE Trans. Instrum. Meas. 61(6), pp. 579–586, 2012.

[2] EJ. Candes, 1. Romberg, T. Tao, "Robust uncertainty principles: exact signal reconstruction from highly incomplete frequency information." IEEE Trans. Inf. Theory. 52(2), pp. 489 - 509, 2006.

[3] C. Luo, J. H. McClellan, "Discrete random sampling theory." In Proc. of ICASSP/2013, pp. 5430 - 5434, 2013.

[4] P. D. Hale, C. M.Wang, D. F.Williams, K. A. Remley, J.Wepman, "Compensation of random and systematic timing errors in sampling oscilloscopes." IEEE Trans. Instrum. Meas. 55(6), pp. 2146–2154, 2006.

[5] P. Daponte, L. De Vito, S. Rapuano, "An extension to IEEE Std. 1241 sine fit for analog-to-information converters testing." In Proc. of $I^2$MTC/2015. Pisa, Italy, pp. 1933-1937, 2015.

[6] M. Bertocco, G. Frigo, C. Narduzzi, "High-accuracy frequency estimation in compressive sensing-plus-DFT

spectral analysis." In Proc. of I²MTC/2015. Pisa, Italy, pp. 1668-1671, 2015.

[7] D. Bao, P. Daponte, L. DE Vito, S. Rapuano, "Frequency-domain characterization of random demodulation analog-to-information converters." ACTA IMEKO. 4(1), pp. 111-120, 2015.

[8] E.J. Candes, M.B. Wakin, "An introduction to compressive sampling." IEEE Signal Proc. Magazine. 25, pp. 21–30, 2008.

[9] R. Baraniuk, M. A. Davenport, M. F. Duarte, C. Hegde, J. Laska, M. Sheikh, W. Yin, "An Introduction to Compressive Sensing." Rice University, Houston, Texas, 2013.

[10] D. C. Rife, R. R. Boorstyn, "Multiple tone parameter estimation from discrete-time observations." Bell Syst. Tech. J. 55, pp. 1389-1410, 1976.

[11] V. H. Jain, W. L. Collins, D. C. Davis, "High accuracy analog measurements via interpolated FFT." IEEE Trans. Instrum. Meas. 28(1), pp. 113-122, 1979.

[12] J. Štremfelj, D. Agrež, "'Nonparametric estimation of power quantities in the frequency domain using Rife-Vincent windows." IEEE Trans. Instrum. Meas. 62(8), pp. 2171-2184, 2013.

[13] P. Stoica, R. Moses, "*Spectral analysis of signals*", Prentice-Hall, NJ, USA, 2005.

[14] Standard IEEE-1241-2010, "*IEEE Standard for Terminology and Test Methods for Analog-to-Digital Converters*", 2011.

[15] 54501A Digitizing Osciloscope Programming Reference, 1989, Agilent Technologies.

[16] 33500B Series Waveform Generators – Data Sheet, 5991-0692EN, 2015, Keysight Technologies.